

# $\eta_c$ production at the LHC challenges nonrelativistic-QCD factorization

Mathias Butenschoen, Zhi-Guo He, and Bernd A. Kniehl

*II. Institut für Theoretische Physik, Universität Hamburg,  
Luruper Chaussee 149, 22761 Hamburg, Germany*

(Dated: March 7, 2018)

We analyze the first measurement of  $\eta_c$  production, performed by the LHCb Collaboration, in the nonrelativistic-QCD (NRQCD) factorization framework at next-to-leading order (NLO) in the strong-coupling constant  $\alpha_s$  and the relative velocity  $v$  of the bound quarks including the feeddown from  $h_c$  mesons. Converting the long-distance matrix elements (LDMEs) extracted by various groups from  $J/\psi$  yield and polarization data to the  $\eta_c$  case using heavy-quark spin symmetry, we find that the resulting NLO NRQCD predictions greatly overshoot the LHCb data, while the color-singlet model provides an excellent description.

PACS numbers: 12.38.Bx, 12.39.St, 13.85.Ni, 14.40.Pq

Despite concerted experimental and theoretical efforts ever since the discovery of the  $J/\psi$  meson in the November revolution of 1974 (The Nobel Prize in Physics 1976), the genuine mechanism underlying the production and decay of heavy quarkonia, which are QCD bound states of a heavy quark  $Q = c, b$  and its antiparticle  $\bar{Q}$ , has remained mysterious. The effective quantum field theory of nonrelativistic QCD (NRQCD) [1] endowed with an appropriate factorization theorem [2] arguably constitutes the most probable candidate theory at the present time. This implies a separation of process-dependent short-distance coefficients (SDCs), to be calculated perturbatively as expansions in the strong-coupling constant  $\alpha_s$ , from supposedly universal long-distance matrix elements (LDMEs), to be extracted from experiment. The relative importance of the latter is subject to velocity scaling rules [3], which predict each of the LDMEs to scale with a definite power of the heavy-quark velocity  $v$ . In this way, the theoretical predictions are organized as double expansions in  $\alpha_s$  and  $v$ . A crucial feature of this formalism is that the  $Q\bar{Q}$  pair can at short distances be produced in any Fock state  $n = {}^{2S+1}L_J^{[a]}$  with definite spin  $S$ , orbital angular momentum  $L$ , total angular momentum  $J$ , and color multiplicity  $a = 1, 8$ . In this way, it complements the color-singlet (CS) model (CSM), which only includes the very  ${}^{2S+1}L_J^{[1]}$  state of the physical quarkonium, and thus cures a severe conceptual shortcoming of the latter, namely the existence of uncanceled infrared (IR) singularities beyond  $L = 0$ . However, the CSM does provide IR-finite NLO predictions for  $S$ -wave charmonia, such as the  $\eta_c$  and  $J/\psi$  mesons considered here.

Despite its theoretical rigor, NRQCD factorization has reached the crossroads in the  $J/\psi$  case. While a global fit [4] to the  $J/\psi$  yields measured in hadroproduction, photoproduction,  $\gamma\gamma$  scattering, and  $e^+e^-$  annihilation successfully pins down the leading color-octet (CO) LDMEs,  $\langle\mathcal{O}^{J/\psi}(1S_0^{[8]})\rangle$ ,  $\langle\mathcal{O}^{J/\psi}(3S_1^{[8]})\rangle$ , and  $\langle\mathcal{O}^{J/\psi}(3P_0^{[8]})\rangle$ , in compliance with the velocity scaling rules, the resulting predictions for  $J/\psi$  polarization in hadroproduction are in striking disagreement with measurements at the Fermilab Tevatron and the CERN LHC [5]. Vice versa, fits to data

on  $J/\psi$  yield and polarization in hadroproduction work reasonably well [6–8], but hopelessly fail in comparisons to the world’s data from other than hadronic collisions [9], with transverse momenta up to  $p_T = 10$  GeV.

Very recently, the LHCb Collaboration measured, for the first time, the prompt  $\eta_c$  yield, via  $\eta_c \rightarrow p\bar{p}$  decays [10]. The data were taken at center-of-mass energies  $\sqrt{s} = 7$  and 8 TeV in the forward rapidity range  $2.0 < y < 4.5$  in bins of  $p_T$ . This provides a tantalizing new opportunity to further test NRQCD factorization and, hopefully, to also shed light on the  $J/\psi$  polarization puzzle, the more so as the  $\eta_c$  meson is the spin-singlet partner of the  $J/\psi$  meson, which implies that the LDMEs of the two are related by heavy-quark spin symmetry (HQSS), one of the pillars of NRQCD factorization. The dominant feeddown contribution is due to the radiative decay  $h_c \rightarrow \eta_c\gamma$ . The leading CS and CO Fock states of direct  $\eta_c$  ( $h_c$ ) production are  $1S_0^{[1]}$  at  $\mathcal{O}(v^3)$  and  $1S_0^{[8]}$ ,  $3S_1^{[8]}$ , and  $1P_1^{[8]}$  at  $\mathcal{O}(v^7)$  ( $1P_1^{[1]}$  and  $1S_0^{[8]}$  at  $\mathcal{O}(v^5)$ ).

So far, only incomplete LO calculations were carried out for direct  $\eta_c$  production, excluding the  $1S_0^{[8]}$  contribution [11]. For the reasons explained above, it is an urgent matter of general interest to provide a full-fledged NRQCD analysis of prompt  $\eta_c$  hadroproduction, at NLO both in  $\alpha_s$  and  $v$ , and this is the very purpose of this Letter. From the  $J/\psi$  case, where such systematic investigations already exist [4, 6–8], we know (i) that  $\mathcal{O}(\alpha_s)$  corrections may be sizable, especially in the  ${}^3P_J^{[8]}$  channels, (ii) that  $\mathcal{O}(v^2)$  corrections may be non-negligible [12, 13], and (iii) that feeddown contributions to prompt production may be substantial, reaching 20–30% in the  $\chi_{cJ}$  case [7, 14, 15].

We work in the collinear parton model of QCD implemented in the fixed-flavor-number scheme with  $n_f = 3$  quark flavors active in the colliding protons, which are represented by parton density functions (PDFs) evaluated at factorization scale  $\mu_f$ . At NLO in NRQCD, the

relevant partonic cross sections are given by

$$\begin{aligned}
d\sigma_{\text{prompt}}^{\eta_c} &= \sum_{n=1S_0^{[1]}, 1S_0^{[8]}, 3S_1^{[8]}, 1P_1^{[8]}} \left[ d\sigma^{c\bar{c}[n]} \langle \mathcal{O}^{\eta_c}(n) \rangle \right. \\
&+ d\sigma_{v^2}^{c\bar{c}[n]} \langle \mathcal{P}^{\eta_c}(n) \rangle \left. \right] + \sum_{n=1P_1^{[1]}, 1S_0^{[8]}} \left[ d\sigma^{c\bar{c}[n]} \langle \mathcal{O}^{h_c}(n) \rangle \right. \\
&+ d\sigma_{v^2}^{c\bar{c}[n]} \langle \mathcal{P}^{h_c}(n) \rangle \left. \right] \mathcal{B}(h_c \rightarrow \eta_c \gamma), \quad (1)
\end{aligned}$$

where  $d\sigma^{c\bar{c}[n]}$  are the Born SDCs including their  $\mathcal{O}(\alpha_s)$  corrections,  $d\sigma_{v^2}^{c\bar{c}[n]}$  contain their  $\mathcal{O}(v^2)$  corrections, and  $\langle \mathcal{Q}^h(n) \rangle$  with  $\mathcal{Q} = \mathcal{O}, \mathcal{P}$  and  $h = \eta_c, h_c$  are the appropriate LDMEs. We approximately account for the mass difference between the  $\eta_c$  and  $h_c$  mesons by substituting  $p_T \rightarrow p_T m_{h_c} / m_{\eta_c}$  in the  $h_c$  SDCs. The definitions of the  $\mathcal{O}$  and  $\mathcal{P}$  operators for  $S$ -wave states and the  $\mathcal{O}$  operator for the  $P$ -wave states may be found in Refs. [2, 13]. Analogously, we define the  $\mathcal{P}$  operators of the relevant  $P$ -wave states as

$$\begin{aligned}
\mathcal{P}^{\eta_c}(1P_1^{[8]}) &= \chi^\dagger \left( -\frac{i}{2} \overleftrightarrow{\mathbf{D}}^j \right) T^a \psi(a_{\eta_c}^\dagger a_{\eta_c}) \\
&\times \psi^\dagger T^a \left( -\frac{i}{2} \overleftrightarrow{\mathbf{D}}^j \right) \left( -\frac{i}{2} \overleftrightarrow{\mathbf{D}} \right)^2 \chi + \text{H.c.}, \\
\mathcal{P}^{h_c}(1P_1^{[1]}) &= \chi^\dagger \left( -\frac{i}{2} \overleftrightarrow{\mathbf{D}}^j \right) \psi(a_{h_c}^\dagger a_{h_c}) \\
&\times \psi^\dagger \left( -\frac{i}{2} \overleftrightarrow{\mathbf{D}}^j \right) \left( -\frac{i}{2} \overleftrightarrow{\mathbf{D}} \right)^2 \chi + \text{H.c.} \quad (2)
\end{aligned}$$

The HQSS relationships between the  $\eta_c$  and  $J/\psi$  ( $h_c$  and  $\chi_{c0}$ ) LDMEs, which are exact through  $\mathcal{O}(v^2)$ , read [2]:

$$\begin{aligned}
\langle \mathcal{Q}^{\eta_c}(1S_0^{[1]}/1S_0^{[8]}) \rangle &= \frac{1}{3} \langle \mathcal{Q}^{J/\psi}(3S_1^{[1]}/3S_1^{[8]}) \rangle \\
\langle \mathcal{Q}^{\eta_c}(3S_1^{[8]}) \rangle &= \langle \mathcal{Q}^{J/\psi}(1S_0^{[8]}) \rangle \\
\langle \mathcal{Q}^{\eta_c}(1P_1^{[8]}) \rangle &= 3 \langle \mathcal{Q}^{J/\psi}(3P_0^{[8]}) \rangle \\
\langle \mathcal{Q}^{h_c}(1P_1^{[1]}/1S_0^{[8]}) \rangle &= 3 \langle \mathcal{Q}^{\chi_{c0}}(3P_0^{[1]}/3S_1^{[8]}) \rangle. \quad (3)
\end{aligned}$$

At  $\mathcal{O}(\alpha_s)$ ,  $\langle \mathcal{O}(1S_0^{[1/8]}) \rangle$  turn out to be proportional to  $(1/\epsilon_{\text{UV}} - 1/\epsilon_{\text{IR}}) \langle \mathcal{O}(1P_1^{[1/8]}) \rangle$ , where the poles in  $\epsilon = 2 - d/2$ , with  $d$  being the space-time dimension in dimensional regularization, are of ultraviolet (UV) or IR origin. After appropriate  $\overline{\text{MS}}$  operator renormalization, the renormalized free-quark LDMEs pertaining to the NRQCD matching procedure for calculating the SDCs are given to  $\mathcal{O}(\alpha_s)$  by

$$\begin{aligned}
\langle \mathcal{O}^h(1S_0^{[8]}) \rangle(\mu_\lambda) &= \langle \mathcal{O}^h(1S_0^{[8]}) \rangle_0 - \frac{4\alpha_s(\mu_\lambda)}{3\pi m^2} \left( \frac{4\pi\mu^2}{\mu_\lambda^2} e^{-\gamma_E} \right)^\epsilon \\
&\times \frac{1}{\epsilon_{\text{IR}}} \left[ \frac{C_F}{2C_A} \langle \mathcal{O}^h(1P_1^{[1]}) \rangle + \left( \frac{C_A}{4} - \frac{1}{C_A} \right) \langle \mathcal{O}^h(1P_1^{[8]}) \rangle \right] \\
\langle \mathcal{O}^h(1S_0^{[1]}) \rangle(\mu_\lambda) &= \langle \mathcal{O}^h(1S_0^{[1]}) \rangle_0 - \frac{4\alpha_s(\mu_\lambda)}{3\pi m^2} \left( \frac{4\pi\mu^2}{\mu_\lambda^2} e^{-\gamma_E} \right)^\epsilon \\
&\times \frac{1}{\epsilon_{\text{IR}}} \frac{1}{2C_A} \langle \mathcal{O}^h(1P_1^{[8]}) \rangle, \quad (4)
\end{aligned}$$

where  $\mu_\lambda$  and  $\mu_r$  are the NRQCD and QCD renormalization scales, respectively, and  $\langle \mathcal{O}^h(n) \rangle_0$  are the tree-level LDMEs. The IR poles in Eq. (4) match otherwise uncanceled IR poles produced by the real radiative corrections to the  $P$ -wave SDCs. The  $\mu_\lambda$  dependences of the renormalized LDMEs are then determined by solving  $\mu_\lambda \frac{d}{d\mu_\lambda} \langle \mathcal{O}^h(n) \rangle_0 = 0$  [16]. We do not need to consider NLO corrections to  $P$ -wave LDMEs, since they are proportional to operators beyond  $\mathcal{O}(v^2)$ .

We calculate the  $\mathcal{O}(\alpha_s)$  and  $\mathcal{O}(v^2)$  corrections to the SDCs using the techniques developed in Refs. [13, 17, 18]. The  $\mathcal{O}(\alpha_s)$  corrections to  $1P_1^{[1]}$  state hadroproduction have only recently been calculated in Ref. [19]. We can reproduce the results therein within the uncertainties expected from the phase-space-slicing method. We can trace the only significant difference to the variation of  $\mu_\lambda$  about its default value, which was executed in Ref. [19] only in the SDCs, where it is induced via Eq. (4), but not in the LDMEs. The  $\mathcal{O}(\alpha_s)$  corrections to the  $1S_0^{[1]}$  and  $1P_1^{[8]}$  SDCs as well as the  $\mathcal{O}(v^2)$  corrections to the  $1S_0^{[1]}$ ,  $1P_1^{[1]}$ , and  $1P_1^{[8]}$  SDCs are calculated here for the first time.

In our numerical analysis, we adopt the values  $m_{\eta_c} = 2983.6$  GeV,  $m_{h_c} = 3525.38$  GeV, and  $\text{Br}(h_c \rightarrow \eta_c \gamma) = 51\%$  from Ref. [20], take the charm-quark mass, which we renormalize according to the on-shell scheme, to be  $m_c = 1.5$  GeV, and use the one-loop (two-loop) formula for  $\alpha_s^{(n_f)}(\mu_r)$  with  $n_f = 4$  at LO (NLO). As for the proton PDFs, we use the CTEQ6L1 (CTEQ6M) set [21] at LO (NLO), which comes with an asymptotic scale parameter of  $\Lambda_{\text{QCD}}^{(4)} = 215$  MeV (326 MeV). Our default scale choices are  $\mu_\lambda = m_c$  and  $\mu_r = \mu_f = m_T$  with  $m_T = \sqrt{p_T^2 + 4m_c^2}$  being the charmonium's transverse mass. We in turn adopt two approaches to determine the  $\eta_c$  and  $h_c$  LDMEs. In the first one, we obtain them via Eq. (3) from the  $J/\psi$  and  $\chi_{c0}$  LDME sets determined at NLO, but ignoring relativistic corrections, by four different groups [4, 6–8] from different selections of  $J/\psi$  and  $\chi_{c0}$  production data (see Table I). In those cases where no  $\chi_{cJ}$  or CS  $J/\psi$  LDMEs are available, we omit the corresponding contributions. The observation that direct  $\eta_c$  production almost exclusively proceeds via the  $3S_1^{[8]}$  channel will provide a retroactive justification for that.

In Fig. 1, we analyze the  $\mathcal{O}(\alpha_s)$  and  $\mathcal{O}(v^2)$  corrections to the contributing SDCs for unit LDMEs. We note that the  $\mathcal{O}(\alpha_s)$  corrections turn the  $1P_1^{[1]}$  SDC negative, a feature familiar, for example, from the  $3P_J^{[8]}$  SDC of direct  $J/\psi$  hadroproduction [18]. However, the  $1P_1^{[8]}$  SDC stays positive also after including the  $\mathcal{O}(\alpha_s)$  corrections. As for the  $\mathcal{O}(v^2)$  corrections, we observe that the ratios  $R(n) = d\sigma_{v^2}^{c\bar{c}[n]} m_c^2 / d\sigma_{\text{NLO}}^{c\bar{c}[n]}$  are almost independent of  $p_T$  and of order unity for all  $n$ , except for  $1P_1^{[1]}$ , which confirms that the relativistic corrections are actually of relative order  $\mathcal{O}(v^2)$ .

In Fig. 2, the LHCb data [10] are compared with the

	Butenschön, Kniehl [4]	Chao, Ma, Shao, Wang, Zhang [6]	Gong, Wan, Wang, Zhang [7]	Bodwin, Chung, Kim, Lee [8]
$\langle \mathcal{O}^{J/\psi}({}^3S_1^{[1]}) \rangle / \text{GeV}^3$	1.32	1.16	1.16	
$\langle \mathcal{O}^{J/\psi}({}^1S_0^{[8]}) \rangle / \text{GeV}^3$	$0.0304 \pm 0.0035$	$0.089 \pm 0.0098$	$0.097 \pm 0.009$	$0.099 \pm 0.022$
$\langle \mathcal{O}^{J/\psi}({}^3S_1^{[8]}) \rangle / \text{GeV}^3$	$0.0016 \pm 0.0005$	$0.0030 \pm 0.012$	$-0.0046 \pm 0.0013$	$0.011 \pm 0.010$
$\langle \mathcal{O}^{J/\psi}({}^3P_0^{[8]}) \rangle / \text{GeV}^5$	$-0.0091 \pm 0.0016$	$0.0126 \pm 0.0047$	$-0.0214 \pm 0.0056$	$0.011 \pm 0.010$
$\langle \mathcal{O}^{\chi_0}({}^3P_0^{[1]}) \rangle / \text{GeV}^5$			0.107	
$\langle \mathcal{O}^{\chi_0}({}^3S_1^{[8]}) \rangle / \text{GeV}^3$			$0.0022 \pm 0.0005$	

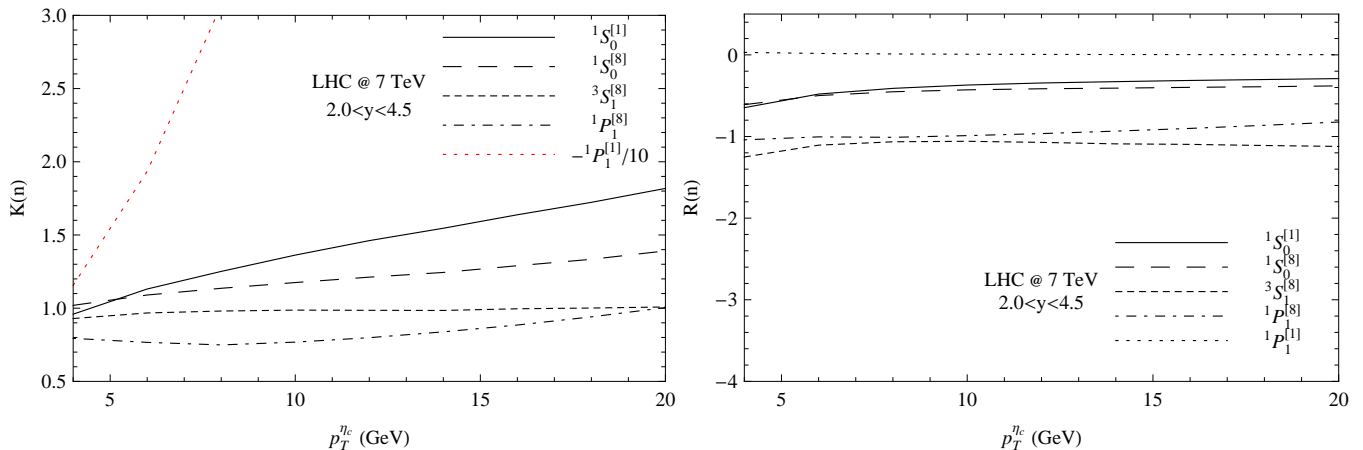
TABLE I: Sets of  $J/\psi$  and  $\chi_{c0}$  LDMEs determined in Refs. [4, 6–8].

FIG. 1: Ratios  $K(n) = d\sigma_{\text{NLO}}^{c\bar{c}[n]} / d\sigma_{\text{LO}}^{c\bar{c}[n]}$  measuring the  $\mathcal{O}(\alpha_s)$  corrections to the SDCs as functions of  $p_T^{\eta_c}$  (left panel). Ratios  $R(n) = d\sigma_{v,2}^{c\bar{c}[n]} m_c^2 / d\sigma_{\text{NLO}}^{c\bar{c}[n]}$  measuring the  $\mathcal{O}(v^2)$  corrections to the SDCs as functions of  $p_T^{\eta_c}$  (right panel). The results for  $n = {}^1P_1^{[1]}$  refer to  $h_c$  production and are evaluated at  $p_T^{h_c} = p_T^{\eta_c} m_{h_c} / m_{\eta_c}$ . The results for  $n = {}^1S_0^{[8]}$  in  $h_c$  production are not shown, but may be obtained from those in  $\eta_c$  production by rescaling as for  $n = {}^1P_1^{[1]}$ . Red color (minus sign in the legend) indicates negative values.

NRQCD and CSM default predictions including  $\mathcal{O}(\alpha_s)$  but excluding  $\mathcal{O}(v^2)$  corrections, evaluated with the four LDME sets in Table I. The error bands shown there are obtained by adding three theoretical errors in quadrature. The first is due to unknown corrections beyond  $\mathcal{O}(\alpha_s)$ , which are estimated by varying  $\mu_\lambda$ ,  $\mu_r$ , and  $\mu_f$  by a factor of two up and down relative to their default values. The second one is due to the fit errors in the LDMEs specified in Table I. The third one is due to the lack of knowledge of the values of  $\langle \mathcal{P}^h(n) \rangle$  and the  $\mathcal{O}(v^2)$  corrections to the HQSS relations (3). Both effects are estimated by evaluating Eq. (1) with  $\langle \mathcal{P}^h(n) \rangle = \xi m_c^2 \langle \mathcal{O}^h(n) \rangle$  and varying  $\xi$  in the range  $-0.5 < \xi < 0.5$ , so that  $\xi$  is of order  $v^2 \approx 0.23$  as obtained from potential model calculations [22].

In Fig. 2, the default NRQCD predictions are also broken down to the individual Fock state contributions. Evidently, the  $h_c$  feeddown contribution is negligible owing to the small  ${}^1P_1^{[1]}$  and  ${}^1S_0^{[8]}$  SDCs, a feature that could not be anticipated without explicit calculation, the more so as the  $\chi_{cJ}$  feeddown contribution to prompt  $J/\psi$  production is quite significant. The most striking feature is, however, that the CSM, which is basically made up just by the  ${}^1S_0^{[1]}$  contribution, yields an almost perfect descrip-

tion of the LHCb data, leaving practically no room for CO contributions. While the  ${}^1S_0^{[8]}$  and  ${}^1P_1^{[8]}$  contributions comply with this condition for all four  $J/\psi$  LDME sets considered, the latter dictate a very sizable  ${}^3S_1^{[8]}$  contribution, which overshoots the LHCb data by up to about one order of magnitude. Even the LDME set that describes the LHCb data best, namely the one of Ref. [4], yields an unacceptable  $\chi^2/\text{d.o.f.}$  value of 257/7 with respect to the default NRQCD predictions. If we take the lower borders of the respective error bands in Fig. 2 as a reference, then  $\chi^2/\text{d.o.f.}$  comes down to 36.7/7, which is still very poor.

In our second approach, we determine the  $\eta_c$  and  $h_c$  LDMEs without recourse to the  $J/\psi$  and  $\chi_{cJ}$  LDMEs, by directly fitting the LHCb data under certain simplifying assumptions. First, we neglect the  $h_c$  feeddown contributions by appealing to their dramatic suppression in Fig. 2. Second, we neglect the  ${}^1S_0^{[8]}$  and  ${}^1P_1^{[8]}$  contributions to direct  $\eta_c$  production because of the  $\mathcal{O}(v^4)$  suppression of their LDMEs relative to the  ${}^1S_0^{[1]}$  one, which is not compensated by an inverse hierarchy in the respective SDCs. In fact, the  ${}^1S_0^{[8]}$  SDCs are only of the same order as the  ${}^1S_0^{[1]}$  ones, while the  ${}^1P_1^{[8]}$  ones are even smaller. We are

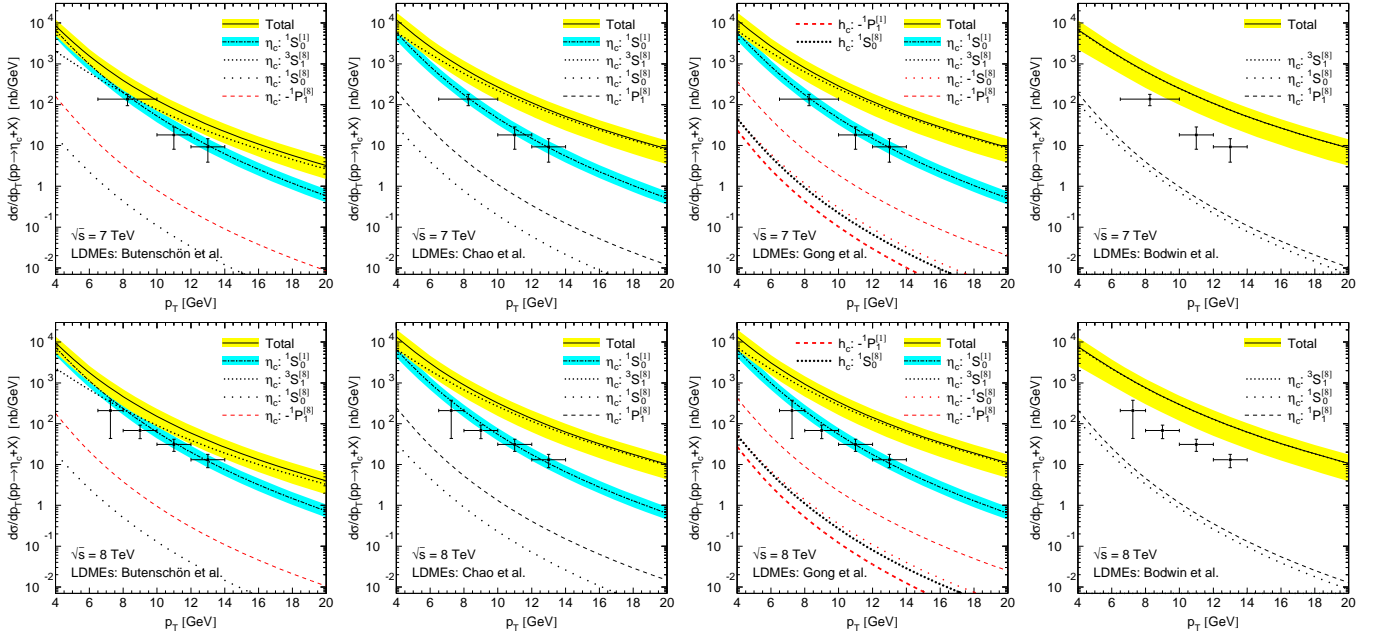


FIG. 2: The LHCb [10] measurements of  $d\sigma/dp_T$  for prompt  $\eta_c$  hadroproduction at  $\sqrt{s} = 7$  TeV (upper panel) and 8 TeV (lower panel) are compared with the default predictions of NRQCD (solid lines) and the CSM (dot-dashed lines) at NLO, but without relativistic corrections, evaluated with the four LDME sets in Table I. The theoretical errors as explained in the text are indicated by the yellow and blue bands, respectively. For comparison, also the default contributions due to the individual Fock states are shown. Red color (minus sign in the legend) indicates negative values.

then left with the  $^1S_0^{[1]}$  and  $^3S_1^{[8]}$  contributions to direct  $\eta_c$  production. As in Table I, we include  $\mathcal{O}(\alpha_s)$  corrections, but neglect  $\mathcal{O}(v^2)$  corrections. Our fitting procedure is as follows. We first determine  $\langle\mathcal{O}^{\eta_c}(^1S_0^{[1]})\rangle$  from the  $\eta_c \rightarrow \gamma\gamma$  partial decay width [23], and then use it as input to fit  $\langle\mathcal{O}^{\eta_c}(^3S_1^{[8]})\rangle$  to the LHCb data. We are entitled to do so, since the difference between the CS LDMEs for production and decay are of  $\mathcal{O}(v^4)$  [2]. In our determination of  $\langle\mathcal{O}^{\eta_c}(^1S_0^{[1]})\rangle$ , we set  $\alpha = 1/137$  and  $\alpha_s(2m_c) = 0.26$ , and adopt the values  $\Gamma_{\eta_c} = (32.3 \pm 1.0)$  MeV and  $\text{Br}(\eta_c \rightarrow \gamma\gamma) = (1.57 \pm 0.12) \times 10^{-4}$  from Ref. [20]. We thus obtain  $\langle\mathcal{O}^{\eta_c}(^1S_0^{[1]})\rangle = (0.24 \pm 0.02)$  GeV<sup>3</sup>, in reasonable agreement with the values of its HQSS counterpart  $\langle\mathcal{O}^{J/\psi}(^3S_1^{[1]})\rangle$  in Table I, and  $\langle\mathcal{O}^{\eta_c}(^3S_1^{[8]})\rangle = (3.3 \pm 2.3) \times 10^{-3}$  GeV<sup>3</sup>, yielding an excellent description of the LHCb data, with  $\chi^2/\text{d.o.f.} = 1.4/6$ . By HQSS, this provides an independent determination of  $\langle\mathcal{O}^{J/\psi}(^1S_0^{[8]})\rangle = \langle\mathcal{O}^{\eta_c}(^3S_1^{[8]})\rangle$ . Observing that this value falls short of the lowest value in Table I, namely the one from Ref. [4], by 6.47 standard deviations, we recover the striking disagreement encountered in our first approach. Such a low value of  $\langle\mathcal{O}^{J/\psi}(^1S_0^{[8]})\rangle$  is in conflict with the ideas behind the high- $p_T$  fits in Refs. [6, 8], which suggest a large  $\langle\mathcal{O}^{J/\psi}(^1S_0^{[8]})\rangle$  value to render the  $^1S_0^{[8]}$  contributions dominant in high- $p_T$   $J/\psi$  hadroproduction and to explain both the  $J/\psi$  yield and polarization observed experimentally. However, unlike the  $J/\psi$  case, the theoretical prediction of direct  $\eta_c$  hadroproduction is well under

control. In fact, there are no large NLO corrections in neither the CS or CO channels, and the  $h_c$  feeddown contributions are also small.

To summarize, we calculated, for the first time, the  $\mathcal{O}(\alpha_s)$  corrections to the  $^1S_0^{[1]}$  and  $^1P_1^{[8]}$  SDCs as well as the  $\mathcal{O}(v^2)$  corrections to the  $^1S_0^{[1]}$ ,  $^1P_1^{[1]}$ , and  $^1P_1^{[8]}$  SDCs. Using the  $\eta_c$  LDMEs derived via HQSS from up-to-date  $J/\psi$  LDMEs [4, 6–8], we demonstrated that the CS contribution alone can nicely describe the new LHCb data on prompt  $\eta_c$  hadroproduction [10], while the full NLO NRQCD predictions yield unacceptably large  $\chi^2/\text{d.o.f.}$  values, of 5.24 and above. On the other hand, the CO contribution is almost exclusively exhausted by the  $^3S_1^{[8]}$  channel, and the  $h_c$  feeddown contribution is negligibly small. This allowed us to directly fit  $\langle\mathcal{O}^{\eta_c}(^3S_1^{[8]})\rangle$  to the LHCb data after determining  $\langle\mathcal{O}^{\eta_c}(^1S_0^{[1]})\rangle$  from  $\Gamma(\eta_c \rightarrow \gamma\gamma)$ , both in NRQCD through  $\mathcal{O}(\alpha_s)$ . Conversion to  $\langle\mathcal{O}^{J/\psi}(^1S_0^{[8]})\rangle$  via HQSS yielded a value that undershoots the expectation from the velocity scaling rules by about one order of magnitude and the respective results from the NLO NRQCD fits to  $J/\psi$  production data currently on the market [4, 6–8] by at least 6.47 standard deviations. Taking for granted that the LHCb results [10] and the HQSS relations (3) can be trusted and observing that the kinematic region probed falls into mid- $p_T$  range, where neither large logarithms  $\ln(p_T^2/m_c^2)$  nor factorization breaking terms are expected, we are led to conclude that either the universality of the LDMEs is in question or that another important ingredient to current

NLO NRQCD analyses has so far been overlooked.

We are grateful to Sergey Barsuk and Maksym Teklishyn for providing us with detailed information about the LHCb data [10]. This work was supported in part by BMBF Grant No. 05 HT6GUA.

*Note added:* After submission, an alternative NRQCD analysis, at NLO in  $\alpha_s$ , of prompt  $\eta_c$  hadroproduction was reported [24], which finds the LHCb  $\eta_c$  data [10] to be consistent with a 2010 set of  $J/\psi$  CO LDMEs [25] fitted to  $J/\psi$  yield data from CDF, in combination with

an upper bound on  $\langle \mathcal{O}^{J/\psi}(1S_0^{[8]}) \rangle$ . We wish to point out that this does not solve the notorious  $J/\psi$  polarization puzzle. In fact, this LDME set drives the polarization variable  $\lambda_\theta$  in the helicity frame to a positive value of approximately 0.4 at large  $p_T$  and central  $y$  values (see first panel of Fig. 8 in [26] and second panel of Fig. 2 in Ref. [24]), in disagreement with the Tevatron and LHC measurements.

- 
- [1] W. E. Caswell and G. P. Lepage, Phys. Lett. B **167**, 437 (1986).
- [2] G. T. Bodwin, E. Braaten, and G. P. Lepage, Phys. Rev. D **51**, 1125 (1995); **55**, 5853(E) (1997).
- [3] G. P. Lepage, L. Magnea, C. Nakhleh, U. Magnea, and K. Hornbostel, Phys. Rev. D **46**, 4052 (1992).
- [4] M. Butenschoen and B. A. Kniehl, Phys. Rev. D **84**, R051501 (2011).
- [5] M. Butenschoen and B. A. Kniehl, Phys. Rev. Lett. **108**, 172002 (2012).
- [6] K. T. Chao, Y. Q. Ma, H. S. Shao, K. Wang, and Y. J. Zhang, Phys. Rev. Lett. **108**, 242004 (2012).
- [7] B. Gong, L. P. Wan, J. X. Wang, and H. F. Zhang, Phys. Rev. Lett. **110**, 042002 (2013).
- [8] G. T. Bodwin, H. S. Chung, U.-R. Kim, and J. Lee, Phys. Rev. Lett. **113**, 022001 (2014).
- [9] M. Butenschoen and B. A. Kniehl, Mod. Phys. Lett. A **28**, 1350027 (2013).
- [10] R. Aaij *et al.* (LHCb Collaboration), arXiv:1409.3612 [hep-ex].
- [11] P. Mathews, P. Poulose, and K. Sridhar, Phys. Lett. B **438**, 336 (1998); S. S. Biswal and K. Sridhar, J. Phys. G **39**, 015008 (2012); A. K. Likhoded, A. V. Luchinsky, and S. V. Poslavsky, arXiv:1411.1247 [hep-ph].
- [12] G. Z. Xu, Y. J. Li, K. Y. Liu, and Y. J. Zhang, Phys. Rev. D **86**, 094017 (2012).
- [13] Zhi-Guo He and B. A. Kniehl, Phys. Rev. D **90**, 014045 (2014).
- [14] F. Abe *et al.* (CDF Collaboration), Phys. Rev. Lett. **79**, 578 (1997).
- [15] R. Aaij *et al.* (LHCb Collaboration), Phys. Lett. B **718**, 431 (2012).
- [16] M. Klasen, B. A. Kniehl, L. N. Mihaila, and M. Steinhauser, Nucl. Phys. B **713**, 487 (2005).
- [17] M. Butenschön and B. A. Kniehl, Phys. Rev. Lett. **104**, 072001 (2010).
- [18] M. Butenschön and B. A. Kniehl, Phys. Rev. Lett. **106**, 022003 (2011).
- [19] J. X. Wang and H. F. Zhang, arXiv:1403.5944 [hep-ph].
- [20] K. A. Olive *et al.* (Particle Data Group), Chin. Phys. C **38**, 090001 (2014).
- [21] J. Pumplin *et al.* (CTEQ Collaboration), JHEP **0207**, 012 (2002).
- [22] G. T. Bodwin, H. S. Chung, D. Kang, J. Lee, and C. Yu, Phys. Rev. D **77**, 094017 (2008); H. K. Guo, Y. Q. Ma, and K. T. Chao, Phys. Rev. D **83**, 114038 (2011).
- [23] R. Barbieri, E. d’Emilio, G. Curci, and E. Remiddi, Nucl. Phys. **B154**, 535 (1979).
- [24] H. Han, Y.-Q. Ma, C. Meng, H.-S. Shao, and K.-T. Chao, arXiv:1411.7350 [hep-ph].
- [25] Y.-Q. Ma, K. Wang, and K.-T. Chao, Phys. Rev. Lett. **106**, 042002 (2011) [arXiv:1009.3655 [hep-ph]].
- [26] H.-S. Shao, H. Han, Y.-Q. Ma, C. Meng, Y.-J. Zhang, and K.-T. Chao, arXiv:1411.3300 [hep-ph].